This article has been accepted for publication in a future issue of this journal, but has not been fully edited. Content may change prior to final publication. Citation information: DOI 10.1109/TUFFC.2018.2850535, IEEE Transactions on Ultrasonics, Ferroelectrics, and Frequency Control

3D velocity and volume flow measurement *in vivo* using speckle decorrelation and 2D high frame rate contrast-enhanced ultrasound

Xiaowei Zhou, Chee Hau Leow, Ethan Rowland, Kai Riemer, Jonathan M. Rubin, Peter D. Weinberg, Mengxing Tang

***Abstract*— Being able to measure 3D flow velocity and volumetric flow rate effectively in the cardiovascular system is valuable but remains a significant challenge in both clinical practice and research. Currently there has not been an effective and practical solution to the measurement of volume flow using ultrasound imaging systems due to challenges in existing 3D imaging techniques and high system cost. In this study, a new technique for quantifying volumetric flow rate from the cross-sectional imaging plane of the blood vessel was developed by using speckle decorrelation, 2D high frame rate imaging with a standard 1D array transducer, microbubble contrast agents, and ultrasound imaging velocimetry (UIV). Through speckle decorrelation analysis of microbubble signals acquired with a very high frame rate and by using UIV to estimate the two in-plane flow velocity components, the third and out-of-plane velocity component can be obtained over time and integrated to estimate volume flow. The proposed technique was evaluated on a wall-less flow phantom in both steady and pulsatile flow. UIV in the longitudinal direction was conducted as a reference. The influences of frame rate, mechanical index, orientation of imaging plane, and compounding on velocity estimation were also studied. In addition, an *in vivo* trial on the abdominal aorta of a rabbit was conducted. The results show that the new system can estimate volume flow with an averaged error of 3.65±2.37% at a flow rate of 360 ml/min and a peak velocity of 0.45 m/s, and an error of 5.03±2.73% at a flow rate of 723 ml/min and a peak velocity of 0.8 m/s. The accuracy of the flow velocity and volumetric flow rate estimation directly depend on the imaging frame rate. With a frame rate of 6000 Hz, a velocity up to 0.8 m/s can be correctly estimated. A higher mechanical index (MI=0.42) is shown to produce greater errors (up to 21.78±0.49%, compared to 3.65±2.37% at MI=0.19). An *in vivo* trial, where velocities up to 1 m/s were correctly measured, demonstrated the potential of the technique in clinical applications.**

***Index Terms*— blood flow rate; e-PIV; microbubbles; speckle decorrelation, ultrafast ultrasound**

I. INTRODUCTION

VOLUMETRIC flow rate is an important indicator for diagnosing many diseases, such as heart failure, carotid stenosis and renal failure [1], [2]; it is also useful for monitoring the changes caused by aging, remodeling, and surgical or pharmacological interventions[3], [4]. Ultrasound imaging, especially Doppler ultrasound, is currently the most common non-invasive modality for volumetric flow measurement, both in clinical practice and research. Other techniques, such as ultrasound imaging velocimetry (UIV), vector Doppler, transverse oscillation beamforming and variants of these[5]–[8], have also been widely investigated in the past two decades. Most of these techniques estimate only the 1D or 2D velocities in the scanning plane, also called 'in-plane', from which the volumetric flow is derived by assuming the blood vessels have a circular cross section with symmetric flow profiles. This assumption can be far from true in the cardiovascular system.

A method to measure the out-of-plane velocity based on Doppler imaging and its intrinsic spectral broadening was introduced [9], but it still requires knowledge of the angle between the flow and the elevational direction of the transducer, which is hard to obtain in practice. In recent years, many studies have endeavoured to develop 3D flow imaging methods with a 2D-array ultrasound probe[10], [11]. The challenges for 3D ultrasound imaging are the huge amount of data and the demanding hardware and computational requirements, which make it difficult and costly to implement [12].

One solution that might be able to overcome these limitations is to characterize the time-varying speckle patterns of scattered signals while scanning arteries in the transverse plane (cross-sectional view of the vessel). The acoustic beam generated by the imaging system has a thickness in the elevational direction, and this allows the estimation of motion parallel to the vessel axis if the transducer is positioned to have a transverse view, as this motion will cause speckle decorrelation in the images. Although there have been many studies of speckle decorrelation (SDC) methods for 3D ultrasound imaging[13], [14], blood flow estimation[15]–[18] and the investigation of elastic tissue properties[19], [20], only a few of them focused on estimating the flow velocity or flow rate in the out-of-plane direction[17], [21], [22]. Furthermore, previous speckle decorrelation studies used only conventional, focused ultrasound; consequently, the maximum measurable velocity can only be about 0.2 m/s, which is more than an order of magnitude lower than peak physiological velocities in the cardiovascular system[21]. The

The manuscript was first submitted for review on 22nd January 2018. This work was supported by the British Heart Foundation under Grant PG/16/95/32350. This work is also partially funded by the UK Engineering and Physical Sciences Research Council under Grant EP/M011933/1. (*Corresponding author: Mengxing Tang.*)

X Zhou, CH Leow, E Rowland, K Riemer, PD Weinberg and MX Tang are with the Department of Bioengineering, Imperial College London, London, United Kingdom (email: mengxing.tang@imperial.ac.uk;).

Rubin JM is with Department of Radiology, University of Michigan, Ann Arbor, MI, USA.

This article has been accepted for publication in a future issue of this journal, but has not been fully edited. Content may change prior to final publication. Citation information: DOI 10.1109/TUFFC.2018.2850535, IEEE Transactions on Ultrasonics, Ferroelectrics, and Frequency Control

reason is that in conventional, focused ultrasound the frame rate can only reach a few hundreds per second, and can be much lower if the scanning region is deep. At low frame rates, speckle patterns from two consecutive frames totally decorrelate, or decorrelate to the noise level, if the flow velocity is high. The low frame rate in previous studies hindered the clinical use of the SDC method for volumetric flow rate estimation.

In the last decade, the emergence of plane-wave ultrasound techniques, which can increase the frame rate by up to two orders of magnitude, has greatly expanded the capability of medical ultrasound imaging [23], [24]. High-frame-rate data acquisition is of particular interest for blood flow imaging because it allows the analysis of peak flows with a high temporal resolution.

Here we investigate the hypothesis that high-frame-rate plane wave imaging can overcome the limitation imposed by conventional, focused ultrasound when using the SDC method to measure high velocity flow in the out-of-plane direction. The feasibility of this method was investigated using microbubble contrast agent and a transverse view of the vessel. Measuring in-plane velocity vectors using the UIV method allowed compensation for decorrelation caused by in-plane motions. Factors that may influence the proposed technique were investigated in experiments on a straight, wall-less flow phantom, and an *in vivo* trial of the rabbit aorta was conducted to demonstrate the potential of the technique for future clinical applications.

II. Theory

In medical ultrasound, the displayed image is the result of phase-sensitive detection of backscattered echoes from a roughly ellipsoidal volume known as the resolution cell. Each pixel in the image corresponds to backscattered echoes from the resolution cell. A specific B-mode image may be considered as a speckle pattern. When the scatterers in the resolution cell move, the speckle pattern will change.

When the number of scatterers within the resolution cell is large and the magnitude and phase of each scattering echo are independent of each other, this type of speckle is defined as fully developed. For fully developed speckle, the decorrelation rate caused by scatterer movements follows a Gaussian curve if the resolution cell of the imaging system is approximated as a Gaussian shape. Those movements may come from different directions (axial, lateral and elevational), all leading to decorrelation of the obtained images. By assuming the image formation is separable into factors arising from the three orthogonal directions, the decorrelation rate can then be derived individually for each direction[17], [25]. Here the derivation of decorrelation rate in the elevational direction is summarized and it can be extended to other directions.

For fully developed speckle, the following relation between the autocorrelation function of the echo signal intensities in the elevational direction (as the object moves relative to the probe in the elevational direction) and the imaging system characteristics has been derived as follows[14], as in

$$R_I(\Delta r) = < I_d >^2 \, (1 + \|\rho(\Delta r)\|^2) \tag{1}$$

where $R_I(\Delta r)$ is the autocorrelation of echo signal intensities in the elevational direction with spatial distance Δr (this can be changed to lag in time when the transducer or scatterer is moving over time), $< I_d >$ the mean diffuse intensity which is constant with position[23][24], and $\|\rho(\Delta r)\|^2$ the normalized coherence factor which is related to the system point spread function and ranges from 0 to 1[25], [26]. As $< I_d >$ is constant with position, the relation between $R_I(\Delta r)$ and $\|\rho(\Delta r)\|^2$ can be regarded as proportional. If the correlation of echo signal intensities $R_I(\Delta r)$ is normalized, the following relation can be obtained, as in

$$C_I(\Delta r) \approx \|\rho(\Delta r)\|^2 \tag{2}$$

where $C_I(\Delta r)$ is the normalized $R_I(\Delta r)$ and it can also be calculated as the linear correlation coefficient between two 2D images (or corresponding 2D patches of the images) with a distance of Δr in the elevational direction [25][26].

The $\|\rho(\Delta r)\|^2$ term in equation (1) and (2) is the normalized coherence factor determined by the shape of the sound beam at different positions. More specifically, it is dependent on the corresponding point spread function[14], [25]. For an array transducer, it has been shown that the normalized coherence factor in the Fraunhofer region of the acoustic field can be approximated as a Gaussian curve[14], [27], as in

$$\|\rho(\Delta r)\|^2 \approx e^{\left(\frac{-\Delta r^2}{2\sigma_y^2}\right)} \tag{3}$$

From equation (2) and (3), it is seen that the normalized correlation function of echo signal intensities in the elevational direction for fully developed speckle objects would follow a specific Gaussian curve. The basic concept of this relationship is illustrated in Fig. 1.

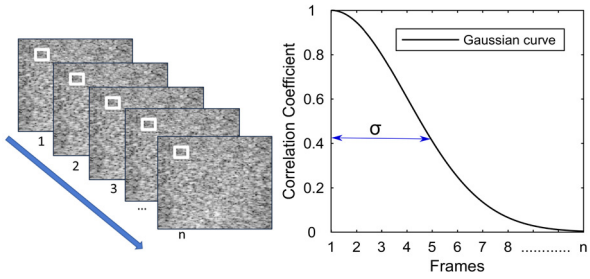

Fig. 1. The intensity values between a series of patches (marked with white boxes) from B-mode frames in the elevational direction (frame 1 to frame n) decorrelate and the decorrelation rate follows a Gaussian curve.

The Gaussian curve is position and transducer setting specific. If the transducer settings are fixed, the corresponding curves at different positions can be obtained by calibration with a speckle phantom using the equation, as in

$$C_{I\_cali}(n) = e^{\frac{-(n\cdot\Delta d)^2}{2\sigma_y^2}} \tag{4}$$

where $C_{I\_cali}(n)$ is the correlation coefficient between B-mode frames from the speckle phantom within the region of interest, n the frame number and Δd the displacement of the phantom

This article has been accepted for publication in a future issue of this journal, but has not been fully edited. Content may change prior to final publication. Citation information: DOI 10.1109/TUFFC.2018.2850535, IEEE Transactions on Ultrasonics, Ferroelectrics, and Frequency Control

between two consecutive frames. With curve fitting, σ_y can be obtained for each specific position. σ_y is also called the beam correlation width (BCW) in the elevational direction. This relation in the elevational direction can be extended to the axial and lateral directions[17], [25], [26], and their corresponding BCWs σ_x and σ_z can also be obtained by the calibration with a speckle phantom.

In blood flow estimation, scatterers moving in three directions (axial, lateral and elevational) would contribute to the decorrelation of the image signal when the transducer is fixed at a position. If the point spread function is assumed to have a Gaussian shape in three directions, the overall decorrelation rate also follows a Gaussian shape[17], as in

$$C_{I\_flow}(n) = e^{\frac{-(v\cdot n\cdot \Delta t)^2}{2\sigma^2}} = e^{\frac{-(n\cdot D\cdot \Delta t)^2}{2}} \quad (5)$$

where $C_{I\_flow}(n)$ is the correlation coefficient between B-mode frames from flow imaging, v the overall velocity, n the frame number, Δt the reciprocal of the ultrasound frame rate and $D = {}^{v}/_{\sigma}$. D is called as the decorrelation value. In this case, D is the overall decorrelation value caused by movements in three directions, and it can be obtained from the B-mode image data by curve fitting. The relation between the overall decorrelation value D, velocity components and BCWs may be represented by equation (6)[17], [22].

$$D^2 = \frac{V_x^2}{\sigma_x^2} + \frac{V_y^2}{\sigma_y^2} + \frac{V_z^2}{\sigma_z^2} \quad (6)$$

In this work, the transducer is placed to have a transverse view of the vessel which means the majority of flow is in the elevational direction (out-of-plane direction). However, there will still be some flow movements in the imaging plane contributing to the overall decorrelation D. To compensate the decorrelation from in-plane movements, V_x and V_z will be tracked by the ultrasound imaging velocimetry (UIV) method with the same image data that is used for estimating the decorrelation value D. In this way, the out-of-plane velocity V_y can then be estimated in equation (6) and the flow rate calculated by integrating over the luminal area.

The UIV algorithm, also known as echo-PIV, is a modification of the conventional particle imaging velocimetry (PIV) algorithm which is based on the 2D cross-correlation of the flow images[29]. In this study, the UIV method was implemented in the same way as it was in our previous studies[5], [30] where some improvements were adopted, including a multiple iterative algorithm, subpixel method, filtering and spurious vector elimination[31].

Microbubbles were used in this study as a contrast agent to enhance the signal-to-noise ratio for the decorrelation method. Microbubbles can be destroyed by the high-intensity acoustic wave from the transducer. The destruction of microbubbles will cause decorrelation of the signal and theoretical models for describing this kind of decorrelation have been reported in studies related to Doppler methods[32], [33]. In the present study, theoretical models for bubble destruction were not investigated, but low MI was used to minimize bubble destruction and high MI was also applied to demonstrate the influence of bubble destruction on the results.

III. Materials and Methods

In this section, a general description of speckle calibration in a speckle phantom is given, followed by flow measurements in flow phantom experiments, a preliminary *in vivo* trial, and an explanation of data processing for the decorrelation method.

A. Calibration of Gaussian curves

To implement the SDC method, the parameter σ in the decorrelation curve must be calibrated for different positions with a speckle phantom[13], [14], [17]. Different imaging settings should be involved in this study. Only a general procedure for calibrating the BCW σ_y for the elevational direction is described in this section; calibrations for the σ_x and σ_z in lateral and axial directions follow a similar procedure.

A speckle phantom was manufactured from 3% agar (W201201, Sigma-Aldrich, United Kingdom) and 1% glass beads (45~90 μm in diameter, Potters Ballotini Ltd, Barnsley, United Kingdom) in de-ionized water. With a clinical ultrasound system (AplioXG, Toshiba Medical Systems, Otawara, Japan), the true speed of sound of this phantom was derived from the measured and known thicknesses.

To calibrate σ_y, the ultrasound probe was clamped to a 3D motorized stage system which moved perpendicular to the scanning plane with a distance of 50 μm between consecutive frames. Fifty B-mode image frames, covering about 2.5 mm in the elevational direction, were obtained. The B-mode images were generated by plane wave imaging. The calibration was performed along the imaging depth, assuming the plane wave beam profile in the lateral direction to be unchanged. Adjacent square patches (10x 10 wavelengths) were defined to calibrate the decorrelation curves at different depths, as shown in Fig. 2. For each depth, there were 50 patches from 50 frames (one from each) in the elevational direction. Those patches contained the same number of pixels and the correlation coefficients between patches at each position were calculated as follows,

$$C_I(i,j) = \frac{\sum_{k=1}^{N}(I_{i,k}-I_{i,mean})(I_{j,k}-I_{j,mean})}{\sqrt{\sum_{k=1}^{N}(I_{i,k}-I_{i,mean})^2}\sqrt{\sum_{k=1}^{N}(I_{j,k}-I_{j,mean})^2}} \quad (7)$$

where N is the number of pixels in each square patch, i and j are frame numbers, $I_{i,k}$ and $I_{j,k}$are the signal intensities of B-mode pixel values, and $I_{i,mean}$ and $I_{j,mean}$ are mean intensity values within the patch. The correlation coefficient $C_I(n)$ in eqn (4) was obtained by averaging all coefficients $C_I(i,j)$ whose frame lag number was n (i.e. when $|i-j| = n$). In this study, a threshold was chosen so that only correlation coefficients greater than 0.3 were used in the Gaussian curve fitting to avoid the influence of noise in the calculation of decorrelations[34]. The calibration was repeated five times and average values were used. These BCW values were fitted to a second order polynomial with respect to imaging depth. The same procedure was followed to calibrate the BCW curve in axial and lateral directions (in-plane directions).

It should be noted that the results are transducer and imaging setting specific and re-calibration is required if image settings change.

This article has been accepted for publication in a future issue of this journal, but has not been fully edited. Content may change prior to final publication. Citation information: DOI 10.1109/TUFFC.2018.2850535, IEEE Transactions on Ultrasonics, Ferroelectrics, and Frequency Control

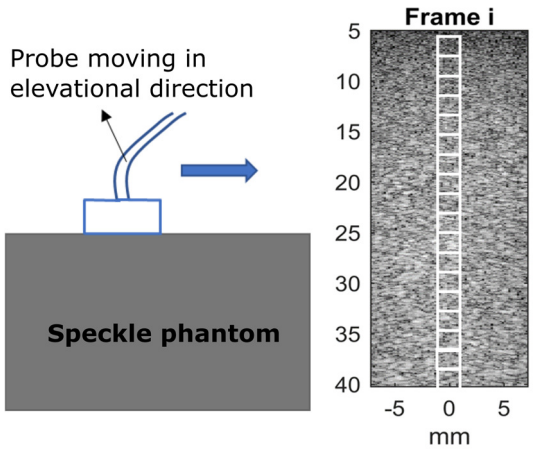

Fig. 2. Transducer moving over a speckle phantom in the elevational direction

B. Flow estimation within a straight wall-less flow phantom

An in-house designed PVA-c based wall-less phantom fabricated in a box was used to mimic a straight blood vessel with diameter of 5.2±0.1 mm (Fig. 3). The PVA-c phantom (15% PVA and 85% water by mass) was made from 3 freeze-thaw cycles of the PVA solution, reported to give tissue-like acoustic properties (speed of sound and attenuation)[35], [36]. The speed of sound of this phantom was calibrated as above. Constant flow was obtained with a gravity feed, and pulsatile flow was generated by a piston pump (Harvard Apparatus, Kent UK). The maximum Reynold's number of the flow in in vitro experiments was 178.The working fluid was water mixed with decafluorobutane microbubbles prepared according to a published procedure[37]. The microbubble solution made in this way has a concentration of about 5 x 10^9 microbubbles per ml[37]. In the present study, the microbubble solution was diluted in gas-equilibrated water to 2 x 10^5 microbubbles per ml[38], a clinically relevant concentration used in previous studies[39]. The Vantage 128 research platform (Verasonics, Redmond, WA, USA) with an L12-3 array probe transmitting at a central frequency of 8MHz was used to collect the high-frame-rate plane wave images from the flow phantom. Except in the mechanical index study, a mechanical index (MI) of 0.19 (calibrated in water) was used in all phantom experiments. Each measurement was repeated three times.

Firstly, the feasibility of the proposed technique was demonstrated in the flow phantom with steady flow. Secondly, the effects of a number of imaging variables were investigated, including frame rate, MI and coherent compounding. Thirdly, the performance of the proposed method under pulsatile flow was studied. In all these experiments, the UIV technique, which has already been well validated [5], [30], was adopted to provide the reference velocity profile in the longitudinal view. For the flow rate, the ground truth was obtained by collecting the effluent over a timed interval.

1) Demonstration of feasibility

Given the limited length of the phantom, a slow flow with peak velocity at about 0.2 m/s was used in order to achieve a well-developed flow at the site of measurement. The L12-3 transducer was positioned to have a transverse view of the vessel and single angle plane-wave imaging at 6000 frames per second (fps) was used for 75 ms to collect 450 B-mode frames for the decorrelation method. Under the same flow condition, the transducer was turned by 90° to have a longitudinal view of the vessel at the same site, to acquire the UIV reference data. The velocity and flow rate estimated by the decorrelation method were compared with the UIV result and the timed-collection result respectively. The UIV and timed-collection methods were also used in the following phantom experiments.

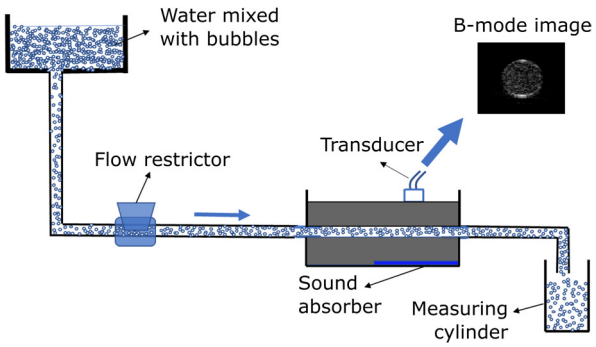

Fig. 3. The setup of the flow phantom

2) Impact of frame rate

To evaluate the impact of imaging frame rate, the same procedures as in the feasibility demonstration were used, but with frame rates ranging from 2000 to 8000 fps in 2000 fps steps to measure a peak velocity of about 0.8 m/s in the phantom.

3) Impact of mechanical index (MI)

Microbubble contrast agents can be disrupted by ultrasound scanning if a high MI is used[40]. The destruction of microbubbles, and/or any additional displacement due to the acoustic radiation force, could change the speckle pattern in the images and lead to decorrelation that is not caused by flow, reducing the accuracy of the decorrelation method in flow estimation. Two MI values (0.19 and 0.42, both calibrated in water) were used to investigate this influence. The flow in the phantom was tuned to have a peak velocity of about 0.45 m/s and the 75-millisecond single angle plane wave data were obtained with a frame rate of 3600 fps.

4) Impact of coherent compounding

Coherent compounding in plane wave imaging can greatly improve the spatial resolution of B-mode images[23]. However, it is not certain whether this would also impact the performance of the decorrelation method. The influence of compounding techniques was studied under steady flow with a peak velocity of about 0.45 m/s. Plane waves were transmitted and received in 3 angles (-5°, 0°, 5°) to form one frame of the compounded image, and the pulse firing rate of 10.8kHz gave a frame rate of 3600 fps. The single angle images were formed from the same data for the compounding but by only taking the zero-angle firing for a fair comparison. Data were collected for 75 ms and used to reconstruct two types of image: a compounded plane wave image from 3 angles and a single angle plane wave image from the zero angle. The same decorrelation method was applied to both type of image.

This article has been accepted for publication in a future issue of this journal, but has not been fully edited. Content may change prior to final publication. Citation information: DOI 10.1109/TUFFC.2018.2850535, IEEE Transactions on Ultrasonics, Ferroelectrics, and Frequency Control

5) Pulsatile flow

A piston pump (Harvard Apparatus 1405 pulsatile blood pump; Harvard Apparatus, Kent, UK) was used to generate pulsatile flow with a frequency of 65 strokes/min. Single angle plane wave data were acquired at a frame rate of 10000 fps for 2 s.

C. In vivo rabbit trial

An *in vivo* experiment was conducted on a male New Zealand White rabbit aged around 10 weeks (2.3kg; Envigo, UK). All procedures complied with the Animals (Scientific Procedures) Act 1989 and were approved by the Animal Welfare and Ethical Review Body of Imperial College London. The rabbit was anaesthetised with Acepromazine (0.5 mg/kg, *im*), Hypnorm (0.3 ml/kg plus 0.1 ml/kg every 45 minutes, *im*) and Midazolam (approx. 0.1 ml/kg every 45 minutes, *iv*). The animal was ventilated via a tracheostomy tube at 40 breaths per minute and body temperature was maintained with a warming plate.

A L11-4v ultrasound probe connected to the Verasonics system was used to obtain a transverse view of the abdominal aorta of the rabbit with the acoustic frequency of 9 MHz. Fur was removed from the scanning sight to improve image quality. Microbubbles (0.05 - 0.1 ml) were injected into the marginal ear vein and the contrast enhanced ultrasound (CEUS) data were collected at 10k fps with an MI of 0.09. Speed of sound was assumed to be 1540 m/s. CEUS data were also obtained by turning the transducer to a longitudinal view, to permit UIV estimation of the reference flow velocity. A singular value decomposition filter was applied to remove the clutter signals in the images in the UIV tracking algorithm[41]. An invasive catheter (Volcano ComboWire XT, Phillips, USA) comprising a forward-facing Doppler ultrasound probe mounted at the tip of a fine wire was inserted via the femoral artery after topical local anesthesia with 1ml Lidocaine and advanced just distal to the imaging site to give another reference velocity (Fig. 4).

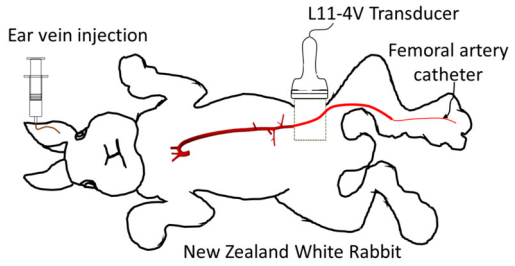

Fig. 4. The *in vivo* experiment on the rabbit abdominal aorta

D. Data processing for flow estimation in the decorrelation method

The lumen was manually identified in the first frame, and automatically segmented in subsequent frames by dynamically tracking the vessel wall with a localized region-based active contour segmentation algorithm[42]. Decorrelation was estimated only within the lumen. A grid consisting of patches with dimensions of 2 x 2 wavelengths, and with 50% overlap (spatial resolution: 192.5 x 192.5um with a central frequency of 8 MHz), were defined within the lumen in each frame. The correlation coefficients between corresponding patches over a certain number of frame pairs (N) were calculated using (7), and then Gaussian curves were fitted for each patch with eqn (5) to estimate the decorrelation value D. This decorrelation value is the average over N frame pairs. For steady flow, N was equal to the duration of collected data multiplied by the frame rate. For pulsatile flow, N was chosen to give a temporal resolution of 200 Hz. It should be noted that the clutter filter is expected to have impact on flow velocity estimation. In this study no clutter filter has been applied to B-mode image.

The same data were also used with the UIV technique for estimating the in-plane velocity vectors V_x and V_z in equation (6). Together with the calibrated beam correlation width σ_x, σ_y and σ_z, the out-of-plane velocity V_y was calculated for each patch position using equation (6). The volumetric flow rate was obtained by integrating estimated out-of-plane velocities over the dynamically segmented luminal area. While in this study 3D velocity vectors were only available on a single plane, based on such vectors the 3D (volumetric) flow rate can be estimated.

IV. Results

A. An example of a calibrated BCW curve from the speckle phantom

An example BCW-depth curve for the elevational direction is shown in Fig. 5. It was acquired using the L12-3 probe transmitting single angle plane waves at a central frequency of 8MHz with MI=0.19. Values of BCW ranged between approximately 200 and 500 μm and increased linearly with depth even though the L12-3 probe has an elevational focal at 20 mm. Similar calibrated BCW curves have been found in other studies[21], [34]. When the depth is over 35 mm, the calibrated BCW values start to fluctuate, which is caused by the low signal-to-noise ratio (SNR) in the deeper area and the incoherence of the beam[34].

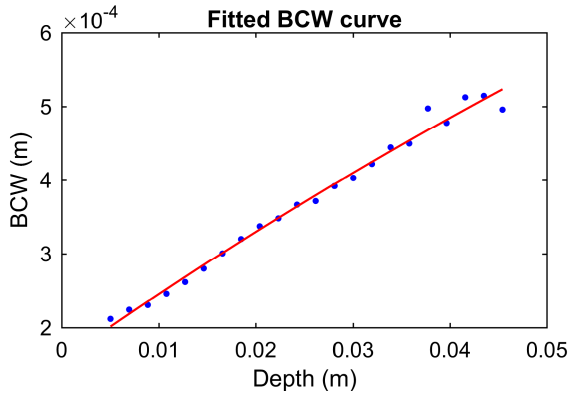

Fig. 5. The calibrated BCW-depth curve obtained using the speckle phantom

B. Flow estimation in the wall-less flow phantom

1) Feasibility

The feasibility of using decorrelation to estimate blood flow in the out-of-plane direction is demonstrated in Fig. 6. Fig. 6a

This article has been accepted for publication in a future issue of this journal, but has not been fully edited. Content may change prior to final publication. Citation information: DOI 10.1109/TUFFC.2018.2850535, IEEE Transactions on Ultrasonics, Ferroelectrics, and Frequency Control

shows that the out-of-plane 2D velocity profile has a shape close to a parabola, as expected from the entrance length. Fig. 6b compares the axial velocity profiles at the center of the vessel from both UIV and SDC methods. They match well, with a root squared mean error of 0.013 (see Table 1). In addition, volumetric flow rate calculated with the new approach had an error of only 0.73±1.92% compared with the timed-collection method (see Table 1).

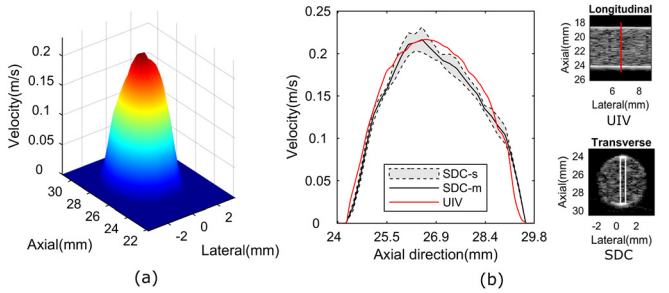

Fig. 6. General demonstration of the decorrelation method. (a): 2D velocity profile in the out-of-plane direction; (b): velocity profile along a line across the center of the vessel from UIV and SDC, the SDC-m curve is the mean profile obtained from a 1-mm wide white box shown on the lower-right picture, the SDC-s grey area represents the standard deviation, and the UIV velocity curve is from the red line shown in the upper-right picture. UIV represents ultrasound imaging velocimetry; SDC represents speckle decorrelation.

2) *Impact of frame rate*

Having a sufficient imaging frame rate was shown to be crucial for accurately estimating the flow velocity when using the new method. When the flow velocity in the phantom was about 0.8 m/s, frame rates of 2000 and 4000 fps both failed to give a correct estimate (Fig. 7a and 7b), compared to the reference UIV measurements. At higher frame rates of 6000 and 8000 fps, the velocity profiles from the SDC and UIV methods matched very well (Fig. 7c and 7d) with RMSEs of 0.037 and 0.043 (see Table 1). When the imaging frame rate is 6000 fps, Figure 8 shows the Gaussian fitting of the decorrelation curve (with the L12-3 probe transmitted at 8 MHz) within a patched-area (2 x 2 wavelengths) near the center of the vessels where their flow rates are different. It takes longer for the pixel intensity values within the patch to decorrelate to a level below a threshold of 0.3 when the flow rate is lower. Estimated volumetric flow rates under the four different frame rates are also compared with the timed-collection measurements in Table 1. When frame rate was sufficiently high, the flow rate estimated by the SDC method had less than 6% error.

3) *Impact of MI*

High MI can cause bubble disruption, and could consequently affect decorrelation signals and the flow velocity estimation. This is shown in Fig. 9, where a lower MI of 0.19 correctly estimated the flow in the out-of-plane direction whereas a large overestimation was found when the MI was increased to 0.42. As a result, volumetric flow rate estimated from the high MI data was also 21.78±0.49 % higher than the reference value from the timed-collection method.

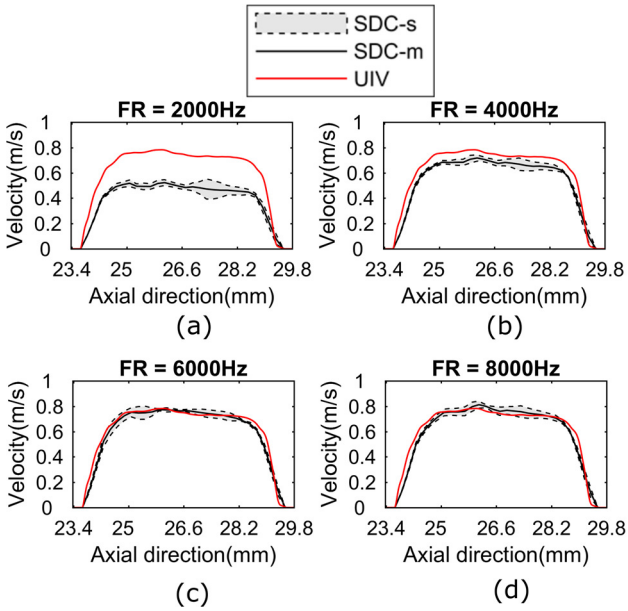

Fig. 7. The influence of frame rate (2000 to 8000 fps) on flow estimation by the decorrelation method, compared to the reference UIV result. UIV, SDC-m and SDC-s were calculated as explained for Fig. 6. UIV represents ultrasound imaging velocimetry; SDC represents speckle decorrelation. fps represents frame per second.

4) *Compound imaging vs single angle imaging*

Although the compounding technique in high-frame-rate plane wave imaging can greatly improve image spatial resolution, Fig. 10 shows compounding the image had little impact on velocity estimation. Flow rates estimated in these two situations were also not too dissimilar (see Table 1). The non-compounded image is therefore preferable for the SDC method since it can provide higher frame rates and estimate higher flow velocities.

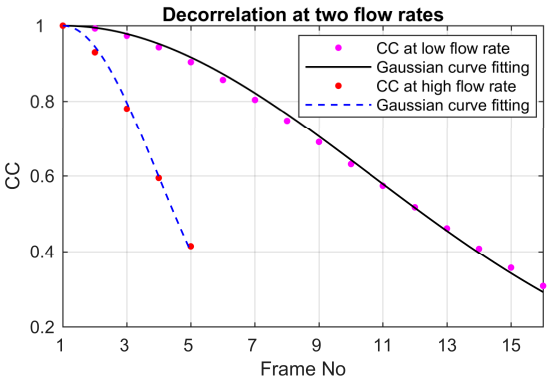

Fig. 8. The Gaussian curve fitting within a patched-area (2x2 wavelengths) near the center of the vessels at two different flow rates corresponding to the two cases in Table 1 (low flow rate is the demo case and high flow rate is the 6000 Hz frame rate case). Imaging frame rates at the two cases are both 6000 Hz. A threshold was used to remove correlation coefficient lower than 0.3 in the curve fitting. CC represents correlation coefficient.

This article has been accepted for publication in a future issue of this journal, but has not been fully edited. Content may change prior to final publication. Citation information: DOI 10.1109/TUFFC.2018.2850535, IEEE Transactions on Ultrasonics, Ferroelectrics, and Frequency Control

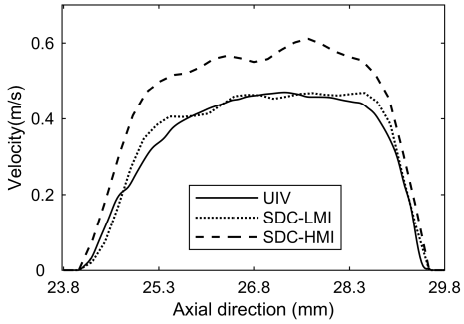

Fig. 9. The influence of MI on flow velocity estimation by SDC, compared to the reference UIV result. SDC-LMI is the result when MI = 0.19 and SDC-HMI is for MI = 0.42. UIV represents ultrasound imaging velocimetry; SDC represents speckle decorrelation; MI represents mechanical index.

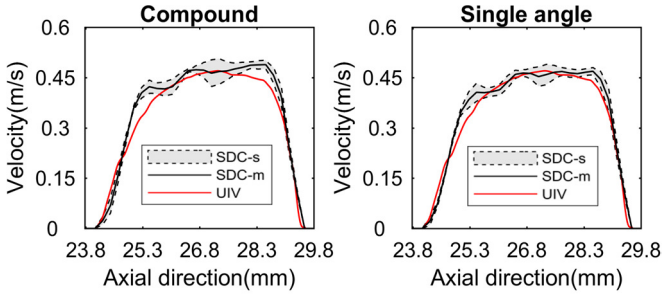

Fig. 10. Flow estimation by SDC using compound imaging or single angle imaging, compared to the reference UIV result. UIV, SDC-m and SDC-s were calculated as explained for Fig. 6. UIV represents ultrasound imaging velocimetry; SDC represents speckle decorrelation.

5) *Pulsatile flow*

The pulsatile flow included reverse flow during the diastolic phase, as shown by the UIV results. Velocity waveforms at the center of the vessel are compared with the UIV data for two cycles in Fig. 11. While the SDC method was able to estimate the magnitude of the flow velocity well compared to the UIV results, it was not able to detect the direction of the flow. This is a limitation of the current SDC method because decorrelation can be caused by scatterer movement in either direction. The movie illustrating the 2D velocity profile in the transverse view within one cycle is provided in Supplementary file 1.

C. *In vivo trial on rabbit*

The CEUS B-mode image of the rabbit's abdominal aorta in the transverse view and the in-plane velocity vectors estimated by UIV at the systolic part of the cycle are shown in Fig. 12. Fig. 13 gives the measured velocity waveforms at the center of the vessel by the SDC method, by the UIV method from the longitudinal view, and by the intravascular catheter. It shows that the SDC method can estimate the flow velocity *in vivo* with a clear and repeatable pulsatile curve that follows the result from both the catheter and UIV very well. A movie is also provided in Supplementary file 2 to illustrate the 2D velocity profile in the transverse view of the aorta within two cycles.

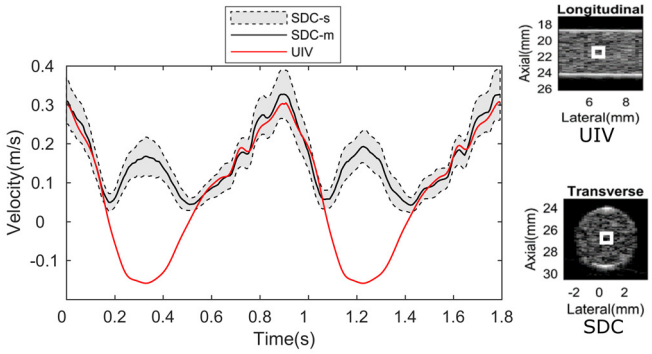

Fig. 11. Velocity profiles obtained by UIV and SDC under pulsatile flow. Both are the mean velocities from the 1-mm square in the vessel center shown by the white boxes in the pictures on the right. UIV represents ultrasound imaging velocimetry; SDC represents speckle decorrelation.

V. Discussion

Effective estimation of 3D flow velocity and volumetric flow would be of great value to clinical practice but is technically challenging. 3D ultrasound imaging technologies are available but significant compromises exist in terms of spatial and temporal resolution, with very high system and probe cost. This study is the first to address that challenge by combining speckle decorrelation, 2D high-frame-rate plane wave ultrasound and microbubble contrast agents. Experiments in the flow phantom and the *in vivo* study of a rabbit aorta show not only that the new approach can accurately estimate flow but also that it substantially extends the upper limit of the measurable flow velocity, to above 1 m/s, compared to the 0.2 m/s obtained in previous studies that employed speckle decorrelation with conventional ultrasound techniques [21]. Such capability enables the technique to be used for measuring physiological flows in arteries.

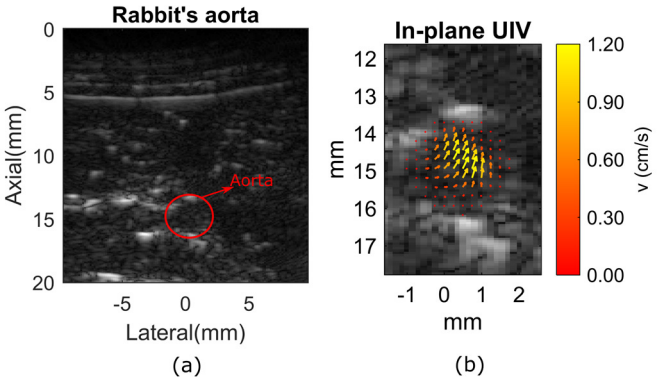

Fig. 12. (a): B-mode image of the rabbit abdominal aorta in the transverse view with contrast agent; (b) the in-plane velocity vectors estimated from UIV at the peak systolic moment in the cycle.

Another novelty of the proposed technique is the use of UIV to estimate the in-plane velocity vectors in the transverse plane, which could be caused by complex vessel geometry and acoustic radiation, with the same data set as that being used for the out-of-plane velocity. In this way, only one scan acquisition is required for estimating all the velocity components required in equation (6), and the in-plane and out-of-plane velocities are

This article has been accepted for publication in a future issue of this journal, but has not been fully edited. Content may change prior to final publication. Citation information: DOI 10.1109/TUFFC.2018.2850535, IEEE Transactions on Ultrasonics, Ferroelectrics, and Frequency Control

TABLE I
ACCURACY OF VELOCITY PROFILES AND FLOW RATES OBTAINED BY SPECKLE DECORRELATION IN THE FLOW PHANTOM

Cases	Variables	RMSE between velocity profiles(m/s) from UIV and SDC	Flow rate from decorrelation (ml/min), mean ± std	Flow rate from timed-collection (ml/min)	Flow rate percentage error (%), mean ± std
Demo	N/A	0.013	121.8±2.3	121	0.73±1.92
Frame rates (fps)	2000	0.222	508.9±6.7	723	-29.6±0.92
	4000	0.072	696.4±4.2	723	-3.7±0.6
	6000	0.037	759.3±19.8	723	5.03±2.73
	8000	0.043	765.7±4.0	723	5.90±0.56
Compound & SA	Compound	0.031	366.0±2.8	360	1.67±0.79
	Single angle	0.023	373.1±8.5	360	3.65±2.37
MI	Low MI	0.023	373.1±8.5	360	3.65±2.37
	High MI	0.111	438.4±1.8	360	21.78±0.49

RMSE represents root mean squared error; UIV represents ultrasound imaging velocimetry; SDC represents speckle decorrelation

obtained at the same time and location. This is more practical and inherently more accurate than the methods where Doppler techniques are used separately to obtain the in-plane velocities [17], [22].

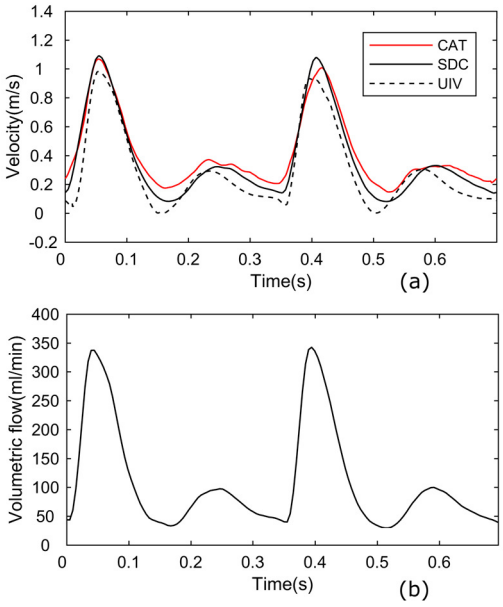

Fig. 13. Measurements of blood velocity in the rabbit aorta (a): SDC curve is the mean velocity within a 1-mm wide square area crossing the center of the aorta in the transverse view. The CAT curve is from the invasive catheter. The UIV curve is the mean velocity within a 1-mm wide square area crossing the center of the aorta in the longitudinal view (b): the volumetric flow rate curve over the aorta calculated from the SDC method. SDC represents the decorrelation method. UIV represents ultrasound imaging velocimetry imaging. CAT represents the catheter.

A key advantage of the proposed technique is that it can be used with any standard ultrasound 1D array probe, without the requirement of 3D sampling in order to calculate the flux through a vessel. This means that as long as the frame rate is sufficiently high, no expensive 3D probes or additional hardware is required. Other key advantages of the approach include that it is also angle independent, flow profile independent except for reverse flow, and vessel geometry independent, making it more practicable for clinical applications. One advantage of using microbubbles is that they are spherical whereas red blood cells are disc shape. Disc-shaped RBCs can stack on top of each other, especially in areas of low shear stress[43]. This phenomenon is known as rouleaux[15], [44], and it can potentially alter the speckle statistics and hence the decorrelation rate.

A sufficiently high frame rate is needed to ensure that the flow is estimated correctly (Fig. 7 and 8). The required rate is largely determined by the beam correlation width (BCW) in the elevational direction, which in this case is only a few hundred micrometers (Fig. 5). In the wall-less phantom, the vessel is centered at a depth of about 25 mm, where the BCW is about 350 μm. It can be assumed that in this case the speckle pattern will be completely decorrelated after scatterers in the sample volume move by a distance of about 700 μm (the BCW is standard deviation of the Gaussian curve as shown in Fig. 1 and it is about half of the curve width). For our velocity of 0.8 m/s, all scatterers move out of the sample volume in about 1ms, corresponding to a frame rate of 1000 fps. In order to obtain at least a few measurement points for calculating the Gaussian curve, the frame rate has to be multiplied by the number of points needed. We found that when the frame rate is increased to 4000 fps, giving about 4 points for the curve fitting, the flow velocity is still underestimated (Fig. 7b). When the frame rate is 6000 fps or above, the velocity can be accurately estimated. Based on the results in this study, the frame rate for the SDC method should be 5-6 times the base frame rate estimated from the reciprocal of the time for all scatterers to pass through the sample volume.

Micobubbles offer significant signal enhancement and are valuable for accurate estimation of velocities, especially in deep tissue and at the lower frequencies used in clinical practice[45], where blood cells are not efficient scatterers. However, the microbubbles are sensitive to MI and can be disrupted. Any disruption of bubbles will add further decorrelation, on top of that produced by flow, and consequently can cause the overestimation of the flow, as shown in Fig. 9. The MI should therefore be set as low as is compatible with achieving a

This article has been accepted for publication in a future issue of this journal, but has not been fully edited. Content may change prior to final publication. Citation information: DOI 10.1109/TUFFC.2018.2850535, IEEE Transactions on Ultrasonics, Ferroelectrics, and Frequency Control

sufficient SNR. The feasibility of using blood cells as the scatterers in this method has not been tested. In principle it could apply to blood cells but we anticipate that the SNR of the blood signal would be much lower. A higher MI value would give a better SNR but is limited by safety issues.

While better spatial resolution can be achieved by coherently compounding images, Fig. 10 shows that such compounding may have a negative impact on velocity estimation. This impact could be caused by the large motion of the scatterers during the compounding scan sequence; the compounding method assumes the imaged object is not moving. Effects caused by flow motion in the compounding method have been reported in other studies[30], [46]. This is actually an advantage for the SDC method because higher frame rates can be achieved without compounding, extending the maximum flow velocity that can be estimated. The frame rate of single angle plane-wave imaging can easily reach 10k for a depth of 35 mm. This means that the flow velocity up to 1.4 m/s can be estimated, based on the discussion in the previous paragraph. However, in Table 1 the flow rate estimated from the compounded data seemed to be more accurate than that from the single angle data. The reason for this is that better segmentation of the lumen area can be achieved due to the better resolution of the compounded images. The segmentation will affect the flow rate estimation since it is directly related to the lumen area.

The volumetric flow rates calculated from the transverse 2D velocity profiles in the constant flow cases showed excellent agreement with the timed-collection measurements (see Table 1). Given appropriate frame rates and MI, the errors were all within 6%. Larger errors occurred at higher flow rates even when the velocities were correctly estimated. This could be caused by error in the segmentation of the luminal area. If the near wall region is not well distinguished by the segmentation algorithm, larger errors in flow rate estimation will happen at higher flow rates, where the velocity profile is blunter. In addition, the decorrelation algorithm calculated velocities in patches of finite size. When patches cross the wall boundary, decorrelations will still happen even if only a small portion of the patch is located within the lumen, which could cause non-zero velocity being estimated outside the lumen area. More work is required to better segment the luminal area in signal angle plane wave images, and to tackle the issue of finite patch size in the algorithm. One possible solution to the segmentation would be to generate a high resolution multi-angel compounded image of the vessel first to better segment the cross-sectional lumen area, before taking the single angle plane wave imaging to estimate the velocity.

To some extent, the overestimation of volumetric flow rate caused by poor segmentation and the patch-based decorrelation algorithm could compensate for the underestimation (Fig. 7a and 7b) of velocity at low frame rates. This may explain why the absolute percentage error at 4000 Hz (-3.7±0.6%) was smaller than at 6000 (5.03±2.73%) and 8000 Hz (5.90±0.56%) – see Table 1.

Another issue arising from using the finite size patch is the spatial velocity gradient which will also cause speckle decorrelation [47]. This extra decorrelation will cause overestimation of velocity in each patch. Although this effect can be mitigated by using high frame rate, as in this study, it cannot be completely removed. Further investigation of this issue is required.

The pulsatile flow used in this study included reverse flow during the diastolic phase of the cycle. However, the SDC method is not able to detect whether flow is forwards or backwards within each of the three directions, but only flow magnitude. This is a current limitation of the decorrelation based method; it will be most accurate in those arteries that have the least reverse flow. However, when it is the volume flow that is of interest, an area without reverse flow could be chosen to conduct the measurement since the mass flow is conserved in the vessel.

In the *in vivo* trial, the pulsatile blood flow velocities in the center of the rabbit aorta estimated with the proposed SDC method were in good agreement with measurements from UIV and catheter. This also proved that the SDC method is capable of accurately detecting flow velocities over 1 m/s with an imaging frame rate of 10,000 fps. The velocity waveform from UIV appeared to be slightly lower than the SDC curve, and they were not in phase to some extent. One possibility is that the vessel was squashed while trying to get a good transverse view during scanning, which could lead to a higher velocity. In this case, the estimation of volumetric flow would not be affected. A second possibility is that the discrepancies could be caused by the fact that the data for SDC and UIV were not collected at the same time, and the true blood flow velocity may therefore have varied. This view is supported by the observation that the velocity curve from the invasive catheter matched very well with the SDC curve and these two methods were applied at the same time.

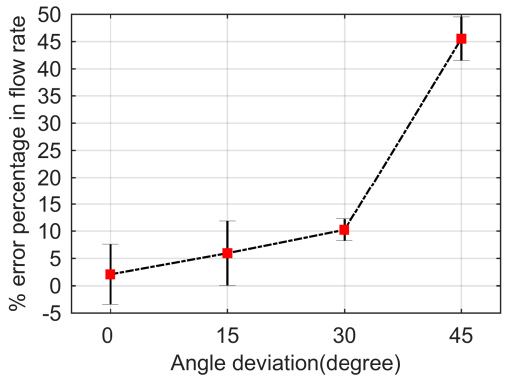

Fig. 14. The error percentage of estimated flow rate when imaging plane is deviated from the perpendicular plane with angles.

In this study, the transducer was placed to give an imaging plane perpendicular to the vessel axis. In practice, it might not be easy to always achieve this in vivo. A trial showed the estimated volumetric flow is indeed affected by the angle deviation from being perpendicular to the flow. The flow rate was increasingly overestimated as the deviation increases, although the error remains below 10% if the deviation is less than 30º (Fig. 14). This result is consistent with a previous study where conventional focused ultrasound imaging was used[17]. One potential reason for the overestimations could be the increased velocity gradient when the flow is not perpendicular to the imaging plane[47]. As pointed out in last paragraph, spatial velocity gradient will cause extra decorrelation [47] which consequently leads to overestimation of flow velocity

and flow rate. It should be achievable to have an angle deviation smaller than 30° in clinical applications to minimize this error.

Finally, we note that our speckle decorrelation method relies on the derived model presented in equation (5) and (6) which do not take imaging aberrations into consideration, so artefacts in the ultrasound imaging, such as clutter signal from the surrounding tissues and variations in the speed of sound, will affect its accuracy. Consequently, the method could be improved if measures, such as clutter filtering, were taken to tackle these artefacts.

VI. Conclusions

A new method using high-frame-rate plane wave imaging, microbubble contrast agents, UIV, and decorrelation analysis was shown to accurately estimate out-of-plane flow velocity and volumetric flow rate both *in vitro* and *in vivo* using a 1D imaging probe. Imaging frame rate and MI both had significant impact on accuracy. It is also necessary to have the ultrasound imaging plane nearly perpendicular to the blood vessel axis while using this method. The technique has a range of potential clinical applications.

Acknowledgments

We are grateful to the British Heart Foundation (Grant no PG/16/95/32350) for funding this project. This work is also partially funded by Engineering and Physical Sciences Research Council in the UK (Grant no EP/M011933/1). We are also grateful to the support of NVIDIA Corporation with the donation of the Titan Xp GPU used for this research.

References

[1] M. L. Robbin *et al.*, "Hemodialysis Arteriovenous Fistula Maturity: US Evaluation," *Radiology*, vol. 225, no. 1, pp. 59–64, 2002.

[2] P. Likittanasombut, P. Reynolds, D. Meads, and C. Tegeler, "Volume flow rate of common carotid artery measured by Doppler method and Color Velocity Imaging Quantification (CVI-Q)," *J. Neuroimaging*, vol. 16, no. 1, pp. 34–38, 2006.

[3] N. Benjamin, A. Calver, J. Collier, B. Robinson, P. Vallance, and D. Webb, "Measuring forearm blood flow and interpreting the responses to drugs and mediators," *Hypertension*, vol. 25, no. 5, pp. 918–923, 1995.

[4] J. R. Weinstein and S. Anderson, "The Aging Kidney: Physiological Changes," *Adv. Chronic Kidney Dis.*, vol. 17, no. 4, pp. 302–307, Jul. 2010.

[5] C. H. Leow, E. Bazigou, R. J. Eckersley, A. C. H. Yu, P. D. Weinberg, and M.-X. Tang, "Flow Velocity Mapping Using Contrast Enhanced High-Frame-Rate Plane Wave Ultrasound and Image Tracking: Methods and Initial in Vitro and in Vivo Evaluation.," *Ultrasound Med. Biol.*, vol. 41, no. 11, pp. 2913–2925, 2015.

[6] B. Dunmire, K. W. Beach, K. H. Labs, M. Plett, and D. E. Strandness, "Cross-beam vector Doppler ultrasound for angle-independent velocity measurements," *Ultrasound Med. Biol.*, vol. 26, no. 8, pp. 1213–1235, 2000.

[7] J. A. Jensen and P. Munk, "A new method for estimation of velocity vectors," *IEEE Trans. Ultrason. Ferroelectr. Freq. Control*, vol. 45, no. 3, pp. 837–851, 1998.

[8] J. A. Jensen, S. I. Nikolov, A. C. H. Yu, and D. Garcia, "Ultrasound Vector Flow Imaging-Part I: Sequential Systems," *IEEE Trans. Ultrason. Ferroelectr. Freq. Control*, vol. 63, no. 11, pp. 1704–1721, 2016.

[9] B.-F. Osmanski, G. Montaldo, and M. Tanter, "Out-of-plane Doppler imaging based on ultrafast plane wave imaging," *IEEE Trans. Ultrason. Ferroelectr. Freq. Control*, vol. 62, no. 4, pp. 625–636, 2015.

[10] S. Holbek, T. L. Christiansen, M. B. Stuart, C. Beers, E. V. Thomsen, and J. A. Jensen, "3-D Vector Flow Estimation with Row-Column-Addressed Arrays," *IEEE Trans. Ultrason. Ferroelectr. Freq. Control*, vol. 63, no. 11, pp. 1799–1814, 2016.

[11] S. Holbek *et al.*, "Ultrasonic 3-D Vector Flow Method for Quantitative In Vivo Peak Velocity and Flow Rate Estimation," vol. 64, no. 3, pp. 544–554, 2017.

[12] J. A. Jensen, S. I. Nikolov, A. C. H. Yu, and D. Garcia, "Ultrasound Vector Flow Imaging-Part II: Parallel Systems," *IEEE Trans. Ultrason. Ferroelectr. Freq. Control*, vol. 63, no. 11, pp. 1722–1732, 2016.

[13] R. J. Housden, A. H. Gee, G. M. Treece, and R. W. Prager, "Sensorless reconstruction of unconstrained freehand 3D ultrasound data," *Ultrasound Med. Biol.*, vol. 33, no. 3, pp. 408–419, 2007.

[14] J.-F. Chen, J. B. Fowlkes, P. L. Carson, and J. M. Rubin, "Determination of scan-plane motion using speckle decorrelation: Theoretical considerations and initial test," *Int J Imaging Sys Technol*, vol. 8, no. 1, pp. 38–44, 1997.

[15] J. M. Rubin *et al.*, "Speckle decorrelation flow measurement with B-mode US of contrast agent flow in a phantom and in rabbit kidney," *Radiology*, vol. 213, no. 2, pp. 429–437, 1999.

[16] W. Li, a. F. W. Steen, C. T. Lancee, I. Cespedes, and N. Bom, "Blood flow imaging and volume flow quantitation with intravascular ultrasound," *Ultrasound Med. Biol.*, vol. 24, no. 2, pp. 203–214, 1998.

[17] J. M. Rubin, T. A. Tuthill, and J. B. Fowlkes, "Volume flow measurement using Doppler and grey-scale decorrelation," *Ultrasound Med. Biol.*, vol. 27, no. 1, pp. 101–109, 2001.

[18] F. A. Lupotti, E. I. Céspedes, and A. F. W. Van Der Steen, "Decorrelation characteristics of transverse blood flow along an intravascular array catheter: Effects of aggregation of red blood cells," *Ultrasound Med. Biol.*, vol. 27, no. 3, pp. 409–417, 2001.

[19] E. Ignacio Céspedes, C. L. de Korte, and A. F. W. Van Der Steen, "Echo decorrelation from displacement gradients in elasticity and velocity estimation," *IEEE Trans. Ultrason. Ferroelectr. Freq. Control*, vol. 46, no. 4, pp. 791–801, 1999.

[20] J. C. Bamber and N. L. Bush, "Freehand Elasticity Imaging using speckle decorrelation rate," *Acoust. Imaging*, vol. 22, no. Edited by P.Tortoli, pp. 285–292, 1995.

[21] D. W. Park *et al.*, "Quantification of Ultrasound Correlation- Based Flow Velocity Mapping and Edge Velocity Gradient Measurement," *Radiol. (J.M.R.), Biomed. Eng.*, 2013.

[22] T. A. Tuthill, J. M. Rubin, and J. B. Fowlkes, "Three-dimensional flow vectors from RF ultrasound signals,"

Proc. SPIE Med. Imag., vol. 4687, no. 2002, pp. 210–217, 2002.

[23] G. Montaldo, M. Tanter, J. Bercoff, N. Benech, and M. Fink, "Coherent Plane Wave Compounding for Very High Frame Rate Ultrasonography and Transient Elastography," *IEEE Trans. Ultrason. Ferroelectr. Freq. Control*, vol. 56, no. 3, pp. 489–506, 2009.

[24] L. Sandrin, S. Catheline, M. Tanter, X. Hennequin, and M. Fink, "Time-Resolved Pulsed Elastography with Ultrafast Ultrasonic Imaging," *Ultrason. Imaging*, vol. 21, no. 4, pp. 259–272, 1999.

[25] R. F. Wagner, S. W. Smith, J. M. Sandrik, and H. Lopez, "Statistics of Speckle in Ultrasound B-Scans," *IEEE Trans. Sonics Ultrason.*, vol. 30, no. 3, pp. 156–163, 1983.

[26] R. F. Wagner, M. F. Insana, and D. G. Brown, "Statistical properties of radio-frequency and envelope detected signal with applications to medical ultrasound," *J. Opt. Soc. Am. A*, vol. 4, no. 5, pp. 910–922, 1987.

[27] R. W. Prager, A. H. Gee, G. M. Treece, C. J. C. Cash, and L. H. Berman, "Sensorless freehand 3-D ultrasound using regression of the echo intensity," *Ultrasound Med. Biol.*, 2003.

[28] P. Hassenpflug, R. W. Prager, G. M. Treece, and A. H. Gee, "Speckle classification for sensorless freehand 3-D ultrasound," *Ultrasound Med. Biol.*, vol. 31, no. 11, pp. 1499–1508, 2005.

[29] R. J. Adrian, "Particle-Imaging Techniques for Experimental Fluid Mechanics," *Annu. Rev. Fluid Mech.*, vol. 23, no. 1, pp. 261–304, 1991.

[30] C. H. Leow and M. X. Tang, "Spatio-Temporal Flow and Wall Shear Stress Mapping Based on Incoherent Ensemble-Correlation of Ultrafast Contrast Enhanced Ultrasound Images," *Ultrasound Med. Biol.*, vol. 44, no. 1, pp. 134–152, 2018.

[31] L. Niu *et al.*, "Ultrasonic particle image velocimetry for improved flow gradient imaging: algorithms, methodology and validation.," *Phys. Med. Biol.*, vol. 55, no. 7, pp. 2103–2120, 2010.

[32] C. Tremblay-Darveau, R. Williams, L. Milot, M. Bruce, and P. N. Burns, "Combined perfusion and doppler imaging using plane-wave nonlinear detection and microbubble contrast agents," *IEEE Trans. Ultrason. Ferroelectr. Freq. Control*, vol. 61, no. 12, pp. 1988–2000, 2014.

[33] C. Tremblay-Darveau, R. Williams, P. S. Sheeran, L. Milot, M. Bruce, and P. N. Burns, "Concepts and Tradeoffs in Velocity Estimation with Plane-Wave Contrast-Enhanced Doppler," *IEEE Trans. Ultrason. Ferroelectr. Freq. Control*, vol. 63, no. 11, pp. 1890–1905, 2016.

[34] T. A. Tuthill, J. F. Krucker, J. B. Fowlkes, and P. L. Carson, "Automated three-dimensional US frame positioning computed from elevational speckle decorrelation," *Radiology*, vol. 209, no. 2, pp. 575–582, 1998.

[35] P. R. Hoskins, "Simulation and Validation of Arterial Ultrasound Imaging and Blood Flow," *Ultrasound Med. Biol.*, vol. 34, no. 5, pp. 693–717, 2008.

[36] D. M. King, C. M. Moran, J. D. McNamara, A. J. Fagan, and J. E. Browne, "Development of a Vessel-Mimicking Material for use in Anatomically Realistic Doppler Flow Phantoms," *Ultrasound Med. Biol.*, vol. 37, no. 5, pp. 813–826, 2011.

[37] P. S. Sheeran, S. Luois, P. A. Dayton, and T. O. Matsunaga, "Formulation and acoustic studies of a new phase-shift agent for diagnostic and therapeutic ultrasound," *Langmuir*, vol. 27, no. 17, pp. 10412–10420, 2011.

[38] H. Mulvana, E. Stride, M. X. Tang, J. V. Hajnal, and R. J. Eckersley, "The Influence of Gas Saturation on Microbubble Stability," *Ultrasound Med. Biol.*, vol. 38, no. 6, pp. 1097–1100, 2012.

[39] M. X. Tang, N. Kamiyama, and R. J. Eckersley, "Effects of nonlinear propagation in ultrasound contrast agent imaging," *Ultrasound Med Biol*, vol. 36, no. 3, pp. 459–466, 2010.

[40] M. Tang, H. Mulvana, T. Gauthier, and A. K. P. Lim, "Quantitative contrast-enhanced ultrasound imaging : a review of sources of variability," *Interface Focus*, no. May, pp. 520–539, 2011.

[41] C. Demené *et al.*, "Speckle decorrelation flow measurement with B-mode US of contrast agent flow in a phantom and in rabbit kidney," *IEEE Trans. Med. Imaging*, vol. 34, no. 11, pp. 2271–2285, 2015.

[42] S. Lankton and A. Tannenbaum, "Localizing Region-Based Active Contours," *IEEE Trans. Image Process.*, vol. 17, no. 11, pp. 2029–2039, Nov. 2008.

[43] B. Sigel, J. Machi, J. C. Beitler, and J. R. Justin, "Red cell aggregation as a cause of blood-flow echogenicity," *Radiology*, vol. 148, no. 3, pp. 799–802, 1983.

[44] K. K. Shung, G. Cloutier, and C. C. Lim, "The Effects of Hematocrit, Shear Rate, and Turbulence on Ultrasonic Doppler Spectrum from Blood," *IEEE Trans. Biomed. Eng.*, vol. 39, no. 5, pp. 462–469, 1992.

[45] K. K. Shung, R. A. Sigelmann, and J. M. Reid, "Scattering of Ultrasound by Blood," *IEEE Trans. Biomed. Eng.*, vol. BME-23, no. 6, pp. 460–467, Nov. 1976.

[46] B. Denarie *et al.*, "Coherent plane wave compounding for very high frame rate ultrasonography of rapidly moving targets," *IEEE Trans. Med. Imaging*, vol. 32, no. 7, pp. 1265–1276, 2013.

[47] B. H. Friemel, L. N. Bohs, K. R. Nightingale, and G. E. Trahey, "Speckle decorrelation due to two-dimensional flow gradients.," *IEEE Trans. Ultrason. Ferroelectr. Freq. Control*, vol. 45, no. 2, pp. 317–27, 1998.